

Figure 2. Extended mesogen resulting from mixing of polymer 1 and stilbazole 2.

Once the mixtures of the interacting liquid-crystalline components were prepared, their mesophases were examined by hot-stage (Mettler FP-52) polarizing microscopy. Polymer 1 and stilbazole ester 2 are miscible over the whole range of composition. Figure 1 shows the phase diagram⁹ of the binary mixture of 1 and 2. For this system, the mixing of 1 and 2 causes a remarkably strong enhancement of the mesophase. This observation is interesting since the isotropization temperatures of binary mixtures usually occur between those of the two individual components.¹⁰ In our case, the mesophase-isotropic transition curve shows a very significant positive deviation from the normal behavior of binary mixtures. For example, the equimolar mixture (1:1 mole ratio of 1/2) displays a mesophase extending from 140 to 252 °C whereas each of the individual components, 1 and 2, shows a transition to isotropic phase at 155 and 216 °C, respectively. The mesomorphic range of the 1:1 mixture is 112 °C while the corresponding ranges for individual components 1 and 2 are 15 and 48 °C, respectively. Even a mixture with only 15 mol % of polymer 1 and 85 mol % of compound 2 shows enhanced mesophase stability to 233 °C.

The mesophase obtained from the 1:1 equimolar mixture was stable to the highest temperature as shown in Figure 1. It is likely that this strong enhancement of the mesophase is in fact caused by the formation of a new and extended mesogenic unit involving the hydrogen-bonded complex shown in Figure 2. If this were not the case and no strong interaction existed between polymer 1 and stilbazole ester 2, the mesophase-isotropic transition curve would be expected to lie close to the dashed straight line in Figure 1.

FT-IR measurements strongly support the existence of the H-bonded complex. The band at 1685 cm⁻¹ observed for 1, which was due to carboxylic acid dimers of polymer 1, is greatly diminished in the 1:1 equimolar mixture, and the band at 1704 cm⁻¹, which appears in its place, seems attributable to the complex formed between the pyridine unit of 2 and the carboxylic acid units of polymer 1.

Homogeneous mesophases possessing similar threaded-type textures were observed for all molar ratios of 1 and 2 in the mixture. These binary mixtures likely form a nematic phase since it is observed that nonstoichiometric mixtures with a high content of 2 (75 or 85 mol %) still form homogeneous mesophases, suggesting that the excess of 2, which, itself, forms a nematic phase, is miscible with the hydrogen-bonded complex of 1 and 2.

Similar effects of mesophase stabilization through intermolecular hydrogen bonding have also been observed by us¹¹ for mixtures in which both components are of low molecular weight such as binary mixtures of an alkoxybenzoic acid and stilbazole ester 2. For example, a 1:1 mixture of 4-butoxybenzoic acid (nematic, 147–160 °C) and stilbazole ester 2 (nematic, 168–216 °C) exhibits a nematic texture up to 237 °C.

p-Alkoxybenzoic acid dimer is known to form a mesophase¹² through the hydrogen bonding of carboxylic acid tail groups. However, our system is significantly different

from the simple acid dimer system since alkoxybenzoic acids always exist as dimers in both the crystalline state and the mesophase, and thus the alkoxybenzoic acid dimer is considered as a single-component mesogen. In our system, it is the mixing of two independent liquid-crystalline components that leads to the formation of a new mesogen through formation of a regular hydrogen-bonded complex. Mesophase stabilization of this magnitude has not been observed for conventional binary mixtures of mesogens. This type of interaction also has great potential in the area of miscibility of liquid-crystalline blends and in the design of novel host-guest liquid-crystalline system.

Acknowledgment. Financial support of this research by IBM Corp.'s Materials and Processing Sciences Program is gratefully acknowledged.

Registry No. 1 (homopolymer), 122408-80-4; 2, 122408-78-0.

References and Notes

- (1) (a) Cifferi, A.; Krigbaum, W. R.; Meyer, R. B., Eds. *Polymer Liquid Crystals*; Academic: New York, 1982. (b) Chapoy, L. L., Ed. *Recent Advances in Liquid Crystalline Polymers*; Elsevier: London, 1985. (c) Blumstein, A., Ed. *Polymeric Liquid Crystals*; Plenum: New York, 1985.
- (2) Jeffrey, G. A. *Acc. Chem. Res.* 1986, 19, 168.
- (3) Aharoni, S. M. *Macromolecules* 1989, 22, 1125, and references therein.
- (4) Polymer 1 was prepared by radical polymerization of 4-[(5-acryloylpentyl)oxy]benzoic acid in DMF (35 wt %) with AIBN (1 mol %). The acrylate monomer was synthesized using a procedure analogous to that described by: Portugall, M.; Ringsdorf, H.; Zentel, R. *Makromol. Chem.* 1982, 183, 2311.
- (5) Stilbazole ester 2 was obtained from *p*-methoxybenzoyl chloride and 4-hydroxy-4'-stilbazole. 4-Hydroxy-4'-stilbazole was synthesized according to the method of Chiang: Chiang, M.-C.; Hartung, W. H. *J. Org. Chem.* 1944, 10, 21.
- (6) Stilbazole ester 2 was reported by: Nash, J. A.; Gray, G. W. *Mol. Cryst. Liq. Cryst.* 1974, 25, 299. However, the nematic range (168–216 °C) we observed was different from their results (140–230 °C). We confirmed the chemical structure of 2 by NMR and FT-IR. Chemical shifts in ¹H NMR spectrum of *trans*-4-alkoxy-4'-stilbazoles were reported by: Bruce, D. W.; Dunmur, D. A.; Lalinde, E.; Maitlis, P. M.; Styring, P. *Liq. Cryst.* 1988, 3, 385. Transition temperatures were measured and confirmed by differential scanning calorimetry (Mettler DSC-20) and hot-stage polarizing microscopy (Mettler FP-52).
- (7) Vivas de Meftahi, M.; Fréchet, J. M. J. *Polymer* 1988, 29, 477.
- (8) Vivas de Meftahi, M.; Fréchet, J. M. J. Manuscript in preparation. Vivas de Meftahi, M. Ph.D. Thesis, University of Ottawa, 1988.
- (9) The range of phase transition where mesophase and isotropic coexisted was about 15 °C. The middle point is plotted in Figure 1.
- (10) Benthack-Thomas, H.; Finkelmann, H. *Makromol. Chem.* 1985, 186, 189.
- (11) Fréchet, J. M. J.; Kato, T.; Kumar, U.; Wilson, P. Manuscript in preparation.
- (12) Gray, G. W.; Jones, B. *J. Chem. Soc.* 1953, 4179.

Takashi Kato and Jean M. J. Fréchet*

Department of Chemistry, Baker Laboratory
Cornell University, Ithaca, New York 14853-1301

Received May 18, 1989;

Revised Manuscript Received July 21, 1989

High Flux X-ray Scattering of Polydiacetylene P4BCMU in Dilute Solution

Polydiacetylenes are prototype conducting polymers. They have many interesting properties, such as a high third-order susceptibility and a high photoconductivity.¹ Applications of polydiacetylenes in materials science and electronics have become significant and have resulted in several commercial products.² Potential uses in polydiacetylenes as an optical memory and information pro-

cessor, utilizing photoinduced isomerization of acetylenic and butatrienic forms and optical nonlinearity, have also been explored.³ It has been found by light scattering^{4,5} and neutron scattering⁶ that the configuration of polydiacetylene depends upon solvent quality; i.e., they are polydisperse coils in good solvent and rodlike aggregates in poor solvent. A reversible conformational change together with a peculiar color change occurs when the solvent quality is changed from good to poor or vice versa. From the results of small-angle light scattering and transient electric birefringence, the overall configuration of rodlike aggregates of polydiacetylene in a poor solvent (toluene) could best be described by a rigid-rod model.^{4,5} However, if one could make a scattering measurement over a wider range of the scattering vector \vec{q} , where its magnitude $q = 4\pi \sin(\theta/2)/\lambda$ with θ and λ being, respectively, the scattering angle and the wavelength of the electromagnetic radiation in the scattering medium, a more detailed picture on the configuration of polydiacetylene in dilute solution could be obtained. Both small-angle X-ray scattering (SAXS) and small-angle neutron scattering (SANS) are appropriate techniques. However, we chose SAXS with synchrotron radiation because of the high X-ray flux. Furthermore, there is no need to deuterate one of the components.

In this paper we report the high flux SAXS of P4BCMU [poly(5,7-dodecadiyne-1,12-bis[(4-butoxycarbonyl)methylurethane]), $(=RC\equiv C\equiv C-CR=)_n$, $R = (CH_2)_4OCONHCH_2COOC_4H_9$] in dilute toluene solution at the State University of New York (SUNY) X-3A2 Beamline, National Synchrotron Light Source (NSLS), Brookhaven National Laboratory (BNL). By combining the SAXS measurements with our light-scattering results, we are able to distinguish the form factors of various models over a scattering vector range of $5 \times 10^{-2} \text{ nm}^{-1} < q < 1.5 \times 10^{-1} \text{ nm}^{-1}$.

P4BCMU ($M_w = 2.4 \times 10^6 \text{ g/mol}$ and $M_w/M_n = 2.1$), courtesy of Dr. D. G. Peiffer at Exxon Research and Engineering Co. was dissolved in toluene at 75°C with a concentration C of $\sim 6 \times 10^{-6} \text{ g/g}$. The solution was cooled to room temperature and kept at room temperature for 2 days before performing the SAXS measurements. The SAXS curve was averaged at room temperatures over a total counting time of $1 \times 10^4 \text{ s}$ using three separate time periods. The SAXS angular range of $1.2\text{--}32 \text{ mrd}$, corresponding to q values of $5 \times 10^{-2}\text{--}1.3 \text{ nm}^{-1}$ ($\lambda = 0.154 \text{ nm}$) was achieved by using a modified Kratky block collimator together with a Braun linear position sensitive detector.⁷ Desmearing was unnecessary since the incident beam had a small cross section of $0.1 \times 2 \text{ mm}^2$ at the sample chamber, and the distance between the sample chamber and the detector was 1.39 m . Background scattering from the slit collimator, the solvent (toluene), and the residual air path between the vacuum chamber and the detector were measured. Excess SAXS from the P4BCMU solute was obtained by subtracting the background scattering from the scattered intensity of the P4BCMU solution after correction for absorption and detector linearity. The recorded data showed that by using the high-flux synchrotron X-ray, the SAXS of P4BCMU solute could be measured even at a very low concentration of $\sim 10^{-6} \text{ g/g}$ with a few hours of accumulation time; but the excess scattered intensity at $q > 1.5 \times 10^{-1} \text{ nm}^{-1}$ was more and more noisy and had only about 100 noisy counts after $\sim 3 \text{ h}$ of accumulation time. In the following analysis we only took the data points at $q \lesssim 1.5 \times 10^{-1} \text{ nm}^{-1}$.

From our light-scattering measurements, we knew that the aggregates had an average radius of gyration (R_g) of

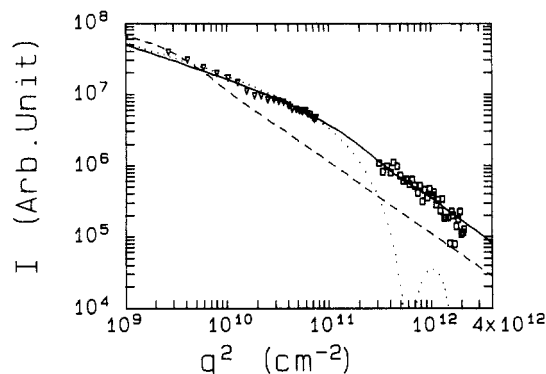


Figure 1. Excess scattered intensity from laser light scattering (hollow inverted triangles measured at $\lambda_0 = 632.8 \text{ nm}$, $C \sim 1 \times 10^{-6} \text{ g/g}$) and SAXS (hollow squares, measured at $\lambda = 0.154 \text{ nm}$, $C \sim 6 \times 10^{-6} \text{ g/g}$) for P4BCMU in dilute toluene solution at room temperatures ($\sim 24^\circ\text{C}$). The three curves represent the theoretical simulations according to various models. Solid line: 14 parallel rods in a $1 \text{ row} \times 14 \text{ columns}$ configuration with the effective diameter of each individual rod being 4 nm and the effective center-to-center distance being 7 nm . Dashed line: an infinitely thin circular disk. Dotted line: a single rod, with the diameter D being 100 nm . The lengths (diameters) of the rod (disk) aggregates were determined by using light-scattering and TEB results based on a rigid-rod model.⁴

the order of a few hundred nanometers.^{4,5} Thus, the SAXS curve covers a q range with $qR_g \gg 1$. Figure 1 shows a log-log plot of I versus q^2 , with I being the excess scattered intensity due to the P4BCMU solute. The hollow squares denote SAXS data while the hollow inverted diamonds denote light-scattering (LS) data. Form factors with different configurations of the aggregates can now be used to fit the entire scattering curve.

In both SAXS and LS measurements, the scattered intensity for a given polydisperse sample is

$$I(\vec{q}) = A \sum_i C_i M_i P_i(\vec{q}) / \sum_i C_i \quad (1)$$

with A being a proportional constant, which has different values for SAXS and LS measurements. C_i , M_i , and $P_i(\vec{q})$ are, respectively, the concentration, the molecular weight, and the form factor of the i th particle. For nonabsorbing particles, the analytical formulae for the form factor P of various particle shapes, such as a rod, an ellipsoid, or a disk, can be found in ref 8. The form factor is particle shape, size, and q value dependent. From the CONTIN⁹ method of Laplace transform inversion of the autocorrelation function of P4BCMU in toluene measured at a small scattering angle by means of dynamic light scattering, the aggregates were found to have a narrow size distribution (with a variance of only 0.04). Thus, we used the average characteristic line width $\bar{\Gamma}$ to perform the structure analysis.

In previous studies^{4,5} dynamic and static light-scattering results yielded an average size of rod aggregates of length $L \sim 0.9 \mu\text{m}$ and thickness $D = 0.1 \mu\text{m}$ and an average aggregation number of ~ 14 . If we were to use a rigid-rod model with the above parameters, the computed scattered intensity profile (denoted by the dotted line in Figure 1) could not agree with the trend of the measured SAXS curve. It should be noted that the same profile could fit the LS data in the small q range. Several other rigid model shapes, including a prolate ellipsoid, an oblate ellipsoid, and a disk with the similar dimensions have been tested. The computed scattered intensity from those models could not even yield the same trend in the small q range. Figure 1 also shows an intensity curve from the disk model (short dashed line). At $qR_g > 1$, SAXS would be much more

sensitive to the details of the particle structure. The cylindrical rigid-rod model obviously needed to be refined if one realized that the particles were aggregated from a bunch of rodlike molecules. A fully straightened P4BCMU molecule would have an average length of 2.2 μm and a thickness of 4 nm,⁴ while the narrowly distributed aggregates had an average length of $\sim 0.9 \mu\text{m}$ with an aggregation number of 14. Thus, it would not be unreasonable to propose a model in which the aggregate particle consisted of a bunch of thin rods parallel to each other. The effective thickness d of each individual rod would be bigger than the 4-nm side length since each individual rod was not fully straightened, but the rod in the same aggregate would be taken as all the same for simplicity. The average length of the aggregates was obtained by using the average translational diffusion coefficient from the CONTIN result, the rotational diffusion coefficient from transient electric birefringence (TEB), and the radius of gyration from static light-scattering measurements [4].

The form factor for such a parallel-rod model could be constructed according to Oster and Riley.¹⁰ By analogy with the scattering from polyatomic gases,¹¹ the form factor (P) of a bundle of similar molecules, each of the form factor S , would be S times the double summation of the intermolecular interference. In the case of n rods, where the centers of the i th and j th rods are at a distance r_{ij} apart

$$P = \frac{S}{n^2} \sum_i \sum_j \exp(iqr_{ij} \cos \alpha) \quad (2)$$

with

$$S = \int_0^{\pi/2} \frac{\pi}{2\nu \cos \beta} \left[J_{1/2}(\nu \cos \beta) \frac{2J_1(\mu \sin \beta)}{\mu \sin \beta} \right]^2 \sin \beta \, d\beta \quad (3)$$

In eq 3, $\nu (=ql/2)$ and $\mu (=qd/2)$ are functions of the length l and the diameter d of each rod. If all rotational orientations about an axis parallel to the lengths of the cylinders are equally probable, each term is integrated between the limits of 0 and 2π for α , we then obtain:

$$P = \frac{S}{n^2} \sum_i \sum_j J_0(qr_{ij}) \quad (4)$$

In eq 2-4, J_i stands for the i th-order Bessel function. To take into account of the fact that the P4BCMU molecules are not fully straightened and that the molecules are not in close contact owing to interparticle repulsion or hydration, we used $r_{ij} = \gamma d$, with γ being a "swelling" parameter.

In the process of connecting the experimental data with model computations, the scaling constants (A ; eq 1) for LS and SAXS were floated in order to yield the best fitting. In a log-scaled plot such an adjustment is related to a vertical shift without changing the shape of the scattering curve. By using different geometrical arrangement of 14 parallel rods, in which the longer cross-section dimension was restricted to $\sim 0.1 \mu\text{m}$, (i.e., the D dimension), we found that, in the small q range, all the computed scattered intensity for rod-shaped particles can be made to agree with the experimental data. However, over the entire q range, i.e., by combining LS data with SAXS data, only an arrangement of 1 row \times 14 columns could yield the best fitting, i.e., the particle configuration is ribbonlike as shown by the solid line in Figure 1. A further more detailed scattering curve covering a broader q range in order to confirm the ribbonlike structure of P4BCMU is under way. If the 14 parallel rods were arranged in a condensed contact

style, the simulated intensity curve would be similar to the one from a single thick rod (Figure 1, dotted line).

In summary, by combining SAXS with LS, the rigid-rod model for P4BCMU aggregates in dilute toluene solution is refined. The P4BCMU molecules in dilute toluene solution form ribbonlike aggregates.

Acknowledgment. The work was supported by the Polymer Program of the National Science Foundation (DMR 8617820) and carried out at the SUNY Beamline supported by the U.S. Department of Energy (DEFG0286-ER45231A001) at the National Synchrotron Light Source, BNL, which is sponsored by the U.S. Department of Energy under Contract DEAC02-76CH00016.

Registry No. P4BCMU (homopolymer), 68777-93-5; P4BCMU (SRU), 76135-61-0.

References and Notes

- (1) Korshak, Y. V.; Medvedeva, T. V.; Ovchinnikov, A. A.; Spektor, V. N. *Nature (London)* **1987**, *326*, 370.
- (2) Prusik, T.; Montesalvo, M.; Wallace, T. *Radiat. Phys. Chem.* **1988**, *31*, 441.
- (3) Hanamura, E.; Itsubo, A. *Pro. SPIE-Int. Soc. Opt. Eng.* **1988**, *824*, 66.
- (4) Xu, R.; Chu, B. *Macromolecules* **1989**, *22*, 3153.
- (5) Xu, R. Ph.D. Dissertation, SUNY at Stony Brook, 1988.
- (6) Rawiso, M.; Aime, J. P.; Fave, J. L.; Schott, M.; Muller, M. A.; Schmidt, M.; Baumgartl, B.; Wegner, G. *J. Phys. Fr.* **1988**, *49*, 861.
- (7) Chu, B.; Wu, D.; Wu, C. *Rev. Sci. Instrum.* **1987**, *58*, 1158.
- (8) Kerker, M. *The Scattering of Light and Other Electromagnetic Radiation*; Academic Press: New York, 1969.
- (9) Provencher, S. W. *Comput. Phys. Comm.* **1982**, *27*, 213; **1982**, *27*, 229.
- (10) Oster, G.; Riley, D. P. *Acta Crystallogr.* **1952**, *5*, 272.
- (11) Debye, P. *Ann. Phys. (Leipzig)* **1915**, *46*, 809.

Benjamin Chu,* Renliang Xu, Yingjie Li, and Dan Q. Wu

Department of Chemistry, State University of New York at Stony Brook, Long Island, New York 11794-3400

Received April 24, 1989;

Revised Manuscript Received July 24, 1989

Studies on the Post-Polymerization of a Liquid-Crystal Polymer with X-Shaped Mesogens

Introduction. An interesting phenomenon was observed in our laboratory during the study of liquid-crystal polymers with X-shaped mesogens: if the sample is annealed for some time at a temperature somewhat higher than its isotropization temperature, the isotropic melt of the sample will become birefringent again. In this article we describe the study of this phenomenon.

The Polymer. The synthesis of liquid-crystal polymers with X-shaped mesogens was first reported by Ringsdorf and co-workers.¹ In this study the polymer has a structure as shown in Figure 1, which was synthesized by solution polycondensation using the diacid dichloride 1,4-bis-[[[4-(chloroformyl)phenyl]oxy]carbonyl]butane (I) and the hydroquinone 2,5-bis[(4-ethoxybenzoyl)oxy]hydroquinone (II) as the monomers. The synthesis of the monomers and the polymers was discussed elsewhere.²

The polymer is a white powder but soluble in THF. The molecular weights of the samples were determined by a Waters 201 GPC instrument using THF as the solvent and polystyrene as the calibration standard. The liquid-crystal properties of the polymer samples were measured by a Perkin-Elmer DSC-4 with a heating rate of 20 $^{\circ}\text{C}/\text{min}$ and by a polarizing microscope with a Leitz 350 heating stage.